Transient Photochemistry, Matrix Isolation, and Molecular Structure of *cis*-Ru(dmpm)$_2$H$_2$ (dmpm = Me$_2$PCH$_2$PMe$_2$)

M. Carmen Nicasio, Robin N. Perutz,* and Paul H. Walton

Department of Chemistry, University of York, Heslington, York YO1 5DD, U.K.

Received December 4, 1996[⊗]

Photolysis of *cis*-Ru(dmpm)$_2$H$_2$ (dmpm = Me$_2$PCH$_2$PMe$_2$) generates the four-coordinate species Ru(dmpm)$_2$, which has been studied by laser flash photolysis and matrix isolation techniques. Ru(dmpm)$_2$ displays weak bands in the visible region of the spectrum. Comparison with analogues containing diphosphines with a CH$_2$CH$_2$ bridge demonstrates the sensitivity of the spectrum to variation of the bite angle, P−Ru−P, of the ring formed by the metal and the diphosphine ligands. The rate constants for the reaction of Ru(dmpm)$_2$ with H$_2$, CO, C$_2$H$_4$, and Et$_3$SiH have been measured. All of the rate constants lie in the range from 2.8×10^8 to 4.9×10^8 dm^3 mol^{-1} s^{-1} at 295 K, showing that Ru(dmpm)$_2$ is very unselective. Ru(dmpm)$_2$ reacts with benzene with complex kinetics, which can be interpreted in terms of a rapid equilibrium between Ru(dmpm)$_2$ and the benzene complex Ru(dmpm)$_2$-(η^2-C$_6$H$_6$). The latter forms the phenyl hydride complex Ru(dmpm)$_2$(Ph)H relatively slowly (rate constant 3.5×10^3 s^{-1}, kinetic isotope effect $k(C_6H_6)/k(C_6D_6) = 1.8$). A single-crystal X-ray structure of *cis*-Ru(dmpm)$_2$H$_2$ shows that the Ru−P bonds *trans* to hydrogen (mean length 2.304(2) Å) are longer than the remaining two Ru−P bonds (mean length 2.282(2) Å). The mean bite angle P−Ru−P of the bridged phosphorus atoms is 72.0°. The unbridged, P−Ru−P angles are 108.0° and 179.2°.

Introduction

The importance of transition metal dihydride complexes lies in the wide variety of catalytic and stoichiometric processes which depend on them.[1] We have concentrated our recent investigations on the photochemistry of dihydride complexes of composition M(dmpe)$_2$H$_2$ (M = Fe, Ru; dmpe = Me$_2$PCH$_2$CH$_2$PMe$_2$).[2] On photolysis, these complexes eliminate hydrogen leading to the formation of 16-electron intermediates M(dmpe)$_2$. By means of laser flash photolysis and matrix isolation techniques we have demonstrated that Ru(dmpe)$_2$ has a square-planar geometry, whereas Fe(dmpe)$_2$ is postulated to have a butterfly structure.

Recently, we have examined the influence of the chelating phosphine ligand on the structure and reactivity of the Ru center in the complexes Ru(R$_2$PCH$_2$CH$_2$PR$_2$)$_2$ (R = C$_2$H$_5$ (depe), C$_6$H$_5$ (dppe), C$_2$F$_5$ (dfepe); we refer to this group of ligands collectively as drpe).[3] Variation of the steric and electronic properties of the phosphine ligands in this series seems to have no significant effect on the structure of the unsaturated species Ru(drpe)$_2$, except for that of dfepe. However, the reactivity of these intermediates depends remarkably on the nature of substituents on the P atoms, increasing in the order Ru(dfepe)$_2$ < Ru(dppe)$_2$ < Ru(depe)$_2$ < Ru(dmpe)$_2$. We have also found that the rate constants for the oxidative addition of H$_2$ are much more sensitive to variation of the phosphine than those of the more stable d^8 square-planar iridium complexes IrCl(CO)(PR$_3$)$_2$ studied previously.[4]

In this paper, we turn our interest to the size of the ring formed by the metal and the chelating phosphine ligand. For this purpose, we have selected a system that contains dmpm, Me$_2$PCH$_2$PMe$_2$, a diphosphine with only one methylene group between the two phosphorus atoms. The compound under study *cis*-Ru(dmpm)$_2$H$_2$ was prepared by Hartwig *et al.*, together with several dialkyl and alkyl hydride complexes of Ru of the general formula Ru(dmpm)$_2$(X)(Y).[5] In this paper, the authors reported that irradiation of *cis*-Ru(dmpm)$_2$H$_2$ in benzene gave the phenyl hydride complex Ru(dmpm)$_2$(Ph)H. They also postulated the formation of the 16-electron intermediate Ru(dmpm)$_2$ in order to explain arene ring exchanges in the complex Ru(dmpm)$_2$(Ph)(H).

Here, we report the photochemistry of *cis*-Ru(dmpm)$_2$H$_2$, in solution and in low-temperature matrices. Photochemical expulsion of H$_2$ from the dihydride precursor generates Ru(dmpm)$_2$. These studies demonstrate that the UV−vis spectrum of the unsaturated fragment is altered substantially by the size of the ring of the metal−ligand system, although its reactivity toward H$_2$, CO, C$_2$H$_4$, and Et$_3$SiH remains similar to that found for the dmpe analogue. On the other hand,

[⊗] Abstract published in *Advance ACS Abstracts,* March 1, 1997.

(1) (a) Pearson, R. G. *Chem. Rev.* **1985**, *85*, 41. (b) *Transition Metal Hydrides*; Dedieu A., Ed; VCH: New York, 1992.

(2) (a) Whittlesey, M. K.; Mawby, R. J.; Osman, R.; Perutz, R. N.; Field, L. D.; Wilkinson, M.; George, M. W. *J. Am. Chem. Soc.* **1993**, *115*, 8627. (b) Hall, C.; Jones, W. D.; Mawby, R. J.; Osman, R.; Perutz, R. N.; Whittlesey, M. K. *J. Am. Chem. Soc.* **1992**, *114*, 7427.

(3) Cronin, L.; Nicasio, M. C.; Perutz, R. N.; Peters, R. G.; Roddick, D. M.; Whittlesey, M. K. *J. Am. Chem. Soc.* **1995**, *117*, 10047.

(4) (a) Chock, P. B.; Halpern, J. *J. Am. Chem. Soc.* **1966**, *88*, 3511. (b) Brady, R.; De Camp, W. H.; Flynn, B. R.; Schneider, M. L.; Scott, J. D.; Vaska, L.; Werneke, M. F. *Inorg. Chem.* **1975**, *14*, 2669. (c) Ugo, R.; Pasini, A.; Fusi, A.; Cenini, S. *J. Am. Chem. Soc.* **1972**, *94*, 7364. (d) Strohmeier, W.; Onoda, T. *Z. Naturforsch.* **1969**, *B24*, 515. (e) Strohmeier, W.; Onoda, T. *Z. Naturforsch.* **1968**, *B23*, 1527. (f) Wilson, M. R.; Liu, H.; Prock, A.; Giering, W. P. *Organometallics* **1993**, *12*, 2044. (g) Wilson, M. R.; Woska, D. C.; Prock, A.; Giering, W. P. *Organometallics* **1993**, *12*, 1742.

(5) Hartwig, J. F.; Andersen, R. A; Bergman, R. G. *Organometallics* **1991**, *10*, 1710.

S0276-7333(96)01018-7 CCC: $14.00

it proves to be considerably more reactive toward benzene, exhibiting complex kinetics. We have also carried out a single-crystal determination of the structure of the dihydride *cis*-Ru(dmpm)$_2$H$_2$ in order to quantify the geometry of the metal−ligand ring. A search reveals only two examples of crystallographic studies of dihydride complexes of Ru containing chelating diphosphines: *cis*-Ru(dppe)$_2$H$_2$ (dppe = $Ph_2PCH_2CH_2PPh_2$)[6] and *cis*-Ru(dfepe)$_2$H$_2$ (dfepe = $(C_2F_5)_2PCH_2CH_2P(C_2F_5)_2$).[7] Both compounds contain a five-membered metal-phosphine ring. We have found only two Ru−dmpm derivatives characterized by X-ray diffraction: the cationic species *trans*-[Ru(dmpm)$_2$(η^1-dmpm)H]PF_6 and the trinuclear complex [Ru$_3$(μ-dmpm)$_3$(dmpm)$_3$Cl$_6$]-C_7H_8·C_2H_5OH.[8,9]

Results

Matrix Photochemistry of *cis*-Ru(dmpm)$_2$H$_2$. *cis*-Ru(dmpm)$_2$H$_2$ is a white solid which sublimes at 60 °C. The UV−vis spectrum of *cis*-Ru(dmpm)$_2$H$_2$ isolated in argon matrices at 12 K was broad and featureless. The IR spectrum showed a group of sharp bands centered at 1769 cm^{-1}, corresponding to Ru−H stretching modes. Vibrations due to the dmpm ligands appeared at lower frequencies.[10]

Broad band UV−vis photolysis (λ > 200 nm) for 15 min caused a 50% depletion of the hydride bands of the starting material. No new ν(Ru−H) absorptions were observed in the region 1700−1900 cm^{-1}. The UV−vis spectrum recorded after photolysis (Figure 1a) showed the presence of weak bands at 330, 440, and 570 nm superimposed on a curve rising steeply toward shorter wavelength. Long wavelength photolysis (λ > 435 nm, ca. 15 h) reduced the intensity of those weak UV−vis absorptions and regenerated the IR bands of the starting dihydride.

The UV−vis spectrum obtained after photolysis of Ru(dmpm)$_2$H$_2$ in methane matrices was the same as in argon matrices, implying that there is no significant interaction between the photoproduct and the matrix.

Laser Flash Photolysis of *cis*-Ru(dmpm)$_2$H$_2$. (a) In Alkane Solvents. The UV−vis spectrum of *cis*-Ru(dmpm)$_2$H$_2$ in heptane solutions is featureless, showing a rise in the absorbance in the UV part of the spectrum. *cis*-Ru(dmpm)$_2$H$_2$ has an extinction coefficient at 308 nm (the laser wavelength) of 1650 dm^3 mol^{-1} cm^{-1}.

Laser flash photolysis (λ_{exc} = 308 nm, pulse width ca. 30 ns, pulse energy ca. 30 mJ) of *cis*-Ru(dmpm)$_2$H$_2$ in heptane (ca. 4 × 10^{-4} mol dm^{-3}) under argon resulted in the rapid formation of a transient (<300 ns) monitored at 400 nm. The transient decayed over 50 μs without returning to the base line, following pseudo-first-order kinetics (k_{obs} = 1.4 × 10^5 s^{-1}, Figure 2). In cyclohexane solutions under argon, the pseudo-first-order rate constant for the decay of the transient species was found to be 4.7 × 10^4 s^{-1}, about three times smaller than that in heptane.

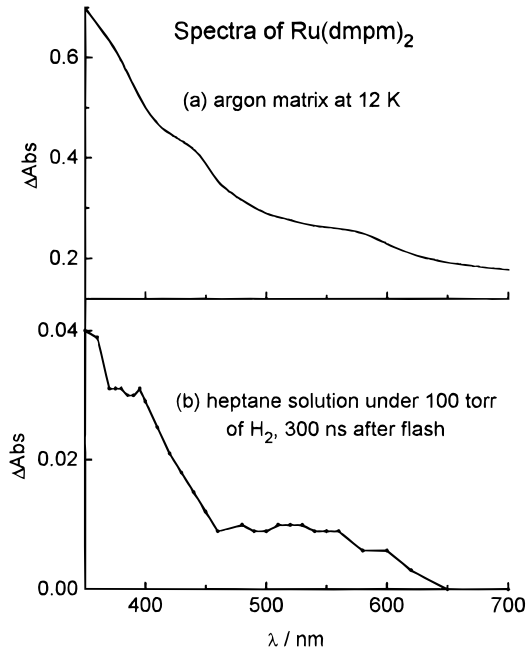

Figure 1. (a) UV−vis spectrum obtained following a 15 min broad-band UV−vis photolysis of *cis*-Ru(dmpm)$_2$H$_2$ in an argon matrix at 12 K. (b) Transient spectrum obtained 300 ns after laser flash photolysis of *cis*-Ru(dmpm)$_2$H$_2$ in heptane solutions under 100 Torr of hydrogen at 295 K.

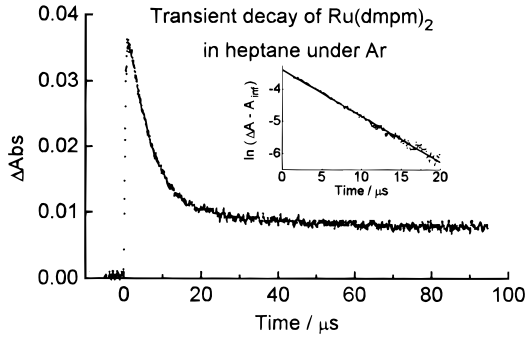

Figure 2. Transient decay following laser flash photolysis (308 nm) of solutions of Ru(dmpm)$_2$H$_2$ in heptane (4 × 10^{-4} mol dm^{-3}) under 1 atm of argon. The inset shows the first-order plot.

The spectrum of the transient formed upon photolysis (Figure 1b) was recorded in heptane under a partial pressure of 100 Torr of H_2 to ensure the maximum reversibility. Comparison to Figure 1a shows that the spectrum in solution resembles that obtained in an argon matrix, with no strong absorptions in the visible part of the spectrum. The long-wavelength band maximum lies at ca. 530 nm, but is poorly defined. There is also a pronounced shoulder at ca. 380 nm.

(b) Quenching by Hydrogen. When laser flash photolysis of *cis*-Ru(dmpm)$_2$H$_2$ in heptane was carried out under partial pressures of H_2 varying from 34 to 175 Torr (made up to a total 760 Torr with argon), an increase in the rate of decay of the transient was observed (monitored at 400 nm). As the partial pressure of H_2 increased, the residual absorbance remaining after decay of the transient grew smaller. A plot of k_{obs} vs $[H_2]$[11] was linear (Figure 3a) and gave a value for the second-order rate constant for the reaction with H_2 of (4.9 ± 0.6) × 10^8 dm^3 mol^{-1} s^{-1} (Table 1).

(6) Pertici, P.; Vitulli, G.; Porzio, W.; Zocchi, M. *Inorg. Chim. Acta* **1979**, *37*, L521.
(7) Koola, J. D.; Roddick, D. M. *J. Am. Chem. Soc.* **1991**, *113*, 1450.
(8) Wong, W. K.; Chiu, K. W.; Wilkinson, G.; Howes, A. J.; Motevalli, M.; Hursthouse, M. B. *Polyhedron* **1985**, *4*, 603.
(9) Van Rooyen, P. H.; Ashworth, T. V.; Hietkamp, S.; Sparrow, N. *Acta Crystallogr., Sect. C. Cryst. Struct. Commun.* **1992**, *48*, 545.
(10) IR bands for Ru(dmpm)$_2$H$_2$ in an argon matrix at 12 K (ν, cm^{-1}): 2970 (m), 2898 (m), 1875 (m), 1777 (m), 1758 (m), 1429 (m), 1420 (m), 1416 (m), 1285 (m), 1275 (s), 1075 (m), 932 (s), 920 (s), 864 (m), 838 (m), 835 (m), 704 (s), 698 (s), 692 (s), 689 (s).

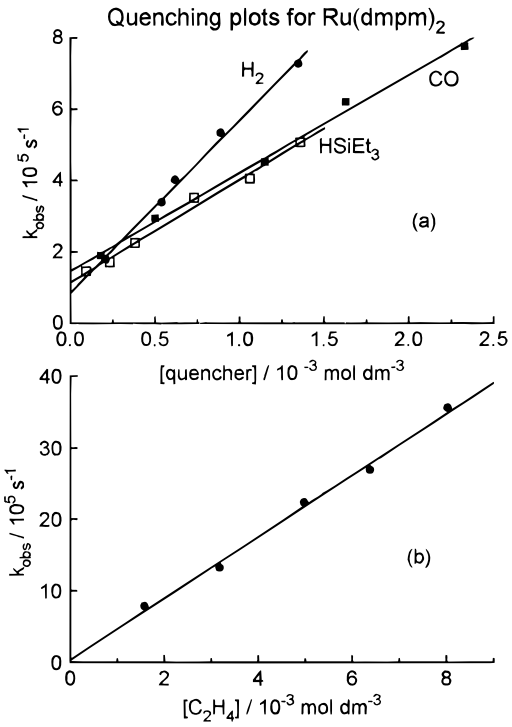

Figure 3. Plots of the pseudo-first-order rate constants for the decay of the transient obtained after laser flash photolysis of $Ru(dmpm)_2H_2$ vs the concentration of added quenching ligands (a) H_2 (●), CO (■) and Et_3SiH (□) and (b) C_2H_4. The best straight lines are shown as full lines through the experimental points.

(c) Quenching by CO, C_2H_4, and Et_3SiH. Laser flash photolysis in heptane under different pressures of CO (11−145 Torr, made up to 760 Torr with argon) again led to the quenching of the transient, but a complete return to the base line was no longer observed. A plot of k_{obs} vs [CO][11] was linear (Figure 3a) and yielded a second-order rate constant of $(2.8 \pm 0.4) \times 10^8$ dm^3 mol^{-1} s^{-1} (Table 1). Similar results were obtained when ethene and Et_3SiH were added to heptane solutions of *cis*-$Ru(dmpm)_2H_2$ (Figure 3b and 3a, Table 1). The temperature dependence for the pseudo-first-order rate constant was measured over the range 294−325 K, with the concentration of $Et_3SiH = 1.1 \times 10^{-3}$ mol dm^{-3}.[12] The activation parameters obtained were as follows: $E_a = (14 \pm 2)$ kJ mol^{-1}, $\Delta H^{\ddagger} = (11 \pm 2)$ kJ mol^{-1}, $\Delta S^{\ddagger} = -(40 \pm 5)$ J mol^{-1} K^{-1} (Figure 4).

(d) Quenching by C_6H_6. Laser flash photolysis of *cis*-$Ru(dmpm)_2H_2$ in neat benzene under argon produced a transient which decayed following pseudo-first-order kinetics ($k_{obs} = 3.6 \times 10^3$ s^{-1}) over 1.5 ms (Figure 5). Contrary to what was expected, the decay observed in benzene is ca. 40 times *slower* than that recorded in heptane (Figure 2). The maximum change in absorbance on flash photolysis of a benzene solution of $Ru(dmpm)_2H_2$ is ca. 50% of that recorded in heptane. Addition of benzene (10^{-4}−11.6 mol dm^{-3}) to heptane solutions of the dihydride resulted in a *decrease* of the observed rate constant of the transient compared to that of neat heptane, reaching a limiting value of ca. 3.5×10^3 s^{-1} when concentrations of C_6H_6 were higher than 0.1 mol dm^{-3} (Figure 6). An inverse plot of $1/k_{obs}$ vs $[C_6H_6]$ gave a straight line over the range from 10^{-4} to 10^{-1} mol dm^{-3} (Figure 7). In order to test for C−H insertion in this reaction, the kinetic isotope effect was measured with neat benzene-d_6 as the solvent. Photolysis of *cis*-$Ru(dmpm)_2H_2$ in benzene-d_6 yielded a transient species that decayed following pseudo-first-order kinetics, and the observed reaction rate constant ($k_{obs} = 1.9 \times 10^3$ s^{-1}) was found to be 1.8 times slower than that in neat C_6H_6. The transient UV−vis spectrum recorded in benzene under 100 Torr of H_2 was similar in form to that obtained in heptane, although the lowest energy band was shifted to 480 nm.

Steady-State Photolysis. The photochemistry of *cis*-$Ru(dmpm)_2H_2$ was also studied in solution with

Table 1. Second-Order Rate Constants[a] for Reactions of $Ru(dmpm)_2$, $Ru(dmpe)_2$, and $Ru(depe)_2$ at 295 K

	k_2/dm^3 mol^{-1} s^{-1}		
quencher	$Ru(dmpm)_2$[b]	$Ru(dmpe)_2$[c]	$Ru(depe)_2$[b]
H_2	$(4.9 \pm 0.6) \times 10^8$	$(6.2 \pm 0.3) \times 10^9$	$(4.4 \pm 0.4) \times 10^8$
CO	$(2.8 \pm 0.4) \times 10^8$	$(4.6 \pm 0.3) \times 10^9$	$(9.1 \pm 0.7) \times 10^7$
C_2H_4	$(4.3 \pm 0.6) \times 10^8$	$(2.2 \pm 0.4) \times 10^8$	$(2.0 \pm 0.7) \times 10^5$
Et_3SiH	$(2.9 \pm 0.5) \times 10^8$	$(2.1 \pm 0.2) \times 10^8$	$(1.1 \pm 0.2) \times 10^5$

[a] Errors are shown at 95% confidence limits. [b] Data recorded in heptane. [c] Data recorded in cyclohexane.

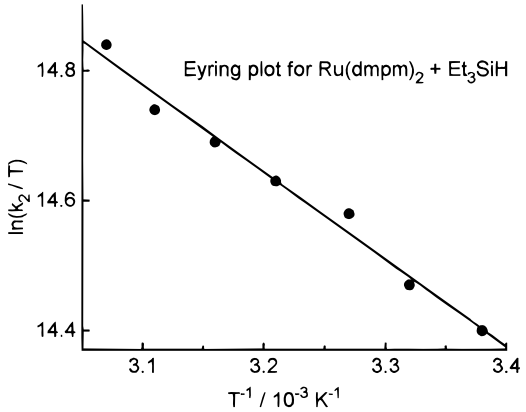

Figure 4. Eyring plot for the temperature dependence of the second-order rate constant for the reaction of the transient following laser flash photolysis of $Ru(dmpm)_2H_2$ in heptane in the presence of 1.1×10^{-3} mol dm^{-3} Et_3SiH. $\Delta H^{\ddagger} = (11 \pm 2)$ kJ mol^{-1}; $\Delta S^{\ddagger} = -(40 \pm 5)$ J mol^{-1} K^{-1}.

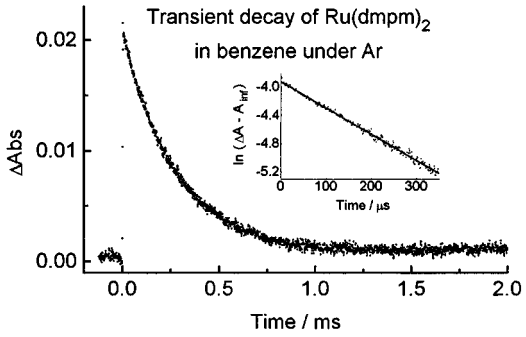

Figure 5. Transient decay following laser flash photolysis (308 nm) of $Ru(dmpm)_2H_2$ in benzene solution under 1 atm of argon, with the corresponding first-order plot as the inset.

(11) Wilhelm, E.; Battino, R. *Chem. Rev.* **1973**, *73*, 1. Gas solubilities were taken as follows: H_2 (heptane 4.7×10^{-3} mol dm^{-3} atm^{-1}, benzene 2.9×10^{-3} mol dm^{-3} atm^{-1}); CO (heptane 1.2×10^{-2} mol dm^{-3} atm^{-1}); ethene (heptane 1.2×10^{-1} mol dm^{-3} atm^{-1}).

(12) Temperature dependence of the rate constants for the reaction of $Ru(dmpe)_2$ with Et_3SiH (1.1×10^{-3} mol dm^{-3}) in heptane, temperature T (K), rate constant k_2 (10^8 dm^3 mol^{-1} s^{-1}): $T = 294$, $k_2 = 5.32$; $T = 301$, $k_2 = 5.77$; $T = 306$, $k_2 = 6.56$; $T = 311$, $k_2 = 7.06$; $T = 316$, $k_2 = 7.60$; $T = 321$, $k_2 = 8.10$; $T = 325$, $k_2 = 9.09$.

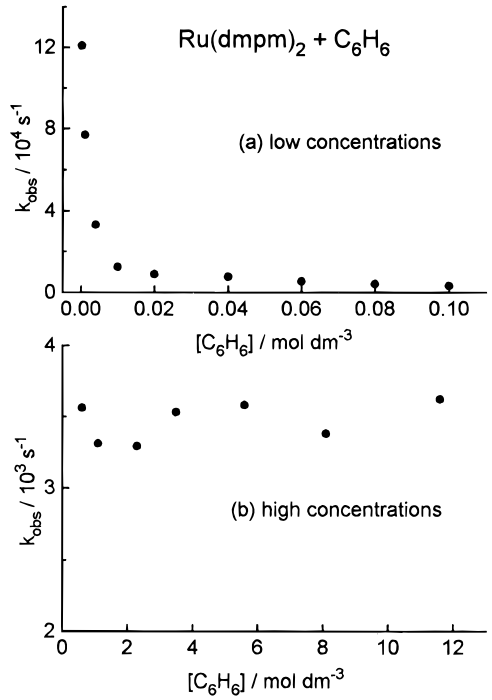

Figure 6. Plots of the pseudo-first-order rate constants for the decay of the transient obtained upon laser flash photolysis of Ru(dmpm)$_2$H$_2$ in hexane/benzene mixtures: (a) [C$_6$H$_6$] = 2 × 10^{-4}−10^{-1} mol dm^{-3} and (b) [C$_6$H$_6$] = 0.6−11.6 mol dm^{-3}.

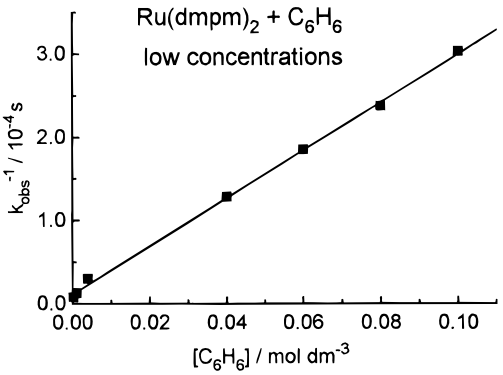

Figure 7. Inverse plot of the pseudo-first-order rate constant for the decay of the transient Ru(dmpm)$_2$ in benzene/hexane mixtures ([C$_6$H$_6$] = 2 × 10^{-4}−10^{-1} mol dm^{-3}).

NMR and IR detection. When a hexane solution of the dihydride was irradiated under 1 atm of CO for ca. 5 min, a new band was observed at 1864 cm^{-1} in the IR spectrum, which was assigned as Ru(dmpm)$_2$(CO) by comparison with those of Ru(dmpe)$_2$CO and Ru(depe)$_2$CO.[2,3]

cis-Ru(dmpm)$_2$H$_2$ was irradiated (λ > 285 nm, ca. 5 h) in a mixture of hexane:Et$_3$SiH (3:1). The mixture was pumped down, and the residue was dissolved in C$_6$D$_6$. A ^{1}H NMR spectrum showed 80% conversion to a product with dmpm and Et$_3$Si resonances and a hydride resonance at δ −8.81, which appeared as a doublet of quartets (J_{PH} = 68.2 and 20.4 Hz). ^{31}P{^{1}H} NMR spectroscopy revealed the presence of an ABMQ spin system (δ_A −19.3, δ_B −25.5, δ_M −33.8, δ_Q −35.1). These NMR data suggest the formation of *cis*-Ru(dmpm)$_2$(H)(SiEt$_3$). Isomerization to a *trans* isomer is not observed, in contrast to the depe analogue.[3]

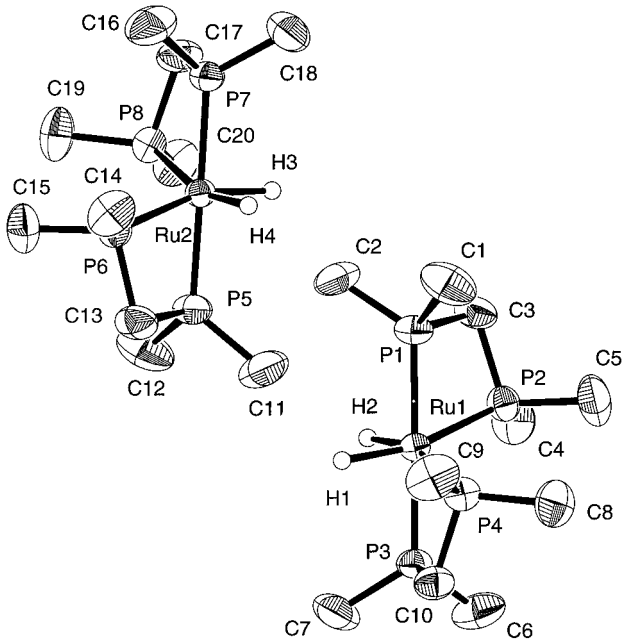

Figure 8. ORTEP diagram of *cis*-Ru(dmpm)$_2$H$_2$ showing the asymmetric unit. Thermal ellipsoids are shown at the 50% level. Hydrogen atoms, except hydrides, are omitted for clarity.

Table 2. Selected Bond Distances (Å) and Angles (deg) for *cis*-Ru(dmpm)$_2$H$_2$ (Enantiomer 1)

Ru(1)−P(1)	2.282(2)	P(2)−C(3)	1.849(6)
Ru(1)−P(2)	2.303(2)	P(2)−C(4)	1.836(6)
Ru(1)−P(3)	2.280(2)	P(2)−C(5)	1.830(6)
Ru(1)−P(4)	2.303(2)	P(3)−C(6)	1.828(7)
Ru(1)−H(1)	1.60(4)	P(3)−C(7)	1.827(6)
Ru(1)−H(2)	1.53(5)	P(3)−C(10)	1.849(6)
P(1)−C(1)	1.829(7)	P(4)−C(8)	1.835(6)
P(1)−C(2)	1.835(6)	P(4)−C(9)	1.831(6)
P(1)−C(3)	1.854(6)	P(4)−C(10)	1.847(6)
P(1)−Ru(1)−P(2)	72.34(7)	H(1)−Ru(1)−P(1)	97(2)
P(1)−Ru(1)−P(3)	179.06(6)	H(1)−Ru(1)−P(2)	164(2)
P(1)−Ru(1)−P(4)	108.90(7)	H(1)−Ru(1)−P(3)	83(2)
P(2)−Ru(1)−P(3)	108.16(7)	H(1)−Ru(1)−P(4)	86(2)
P(2)−Ru(1)−P(4)	107.91(7)	H(2)−Ru(1)−P(1)	87(2)
P(3)−Ru(1)−P(4)	71.75(7)	H(2)−Ru(1)−P(2)	88(2)
P(2)−C(3)−P(1)	93.9(3)	H(2)−Ru(1)−P(3)	92(2)
P(4)−C(10)−P(3)	93.3(3)	H(2)−Ru(1)−P(4)	160(2)

Hartwig *et al.*[5] reported the photochemical reaction of Ru(dmpm)$_2$H$_2$ with benzene-d_6. The reaction led to the formation of *cis*-Ru(dmpm)$_2$(D)(C$_6$D$_5$) after 4 days photolysis at room temperature in a 48% yield. We irradiated a sample of Ru(dmpm)$_2$H$_2$ in C$_6$H$_6$ for 20 h. ^{1}H and ^{31}P{^{1}H} NMR spectra of the residue resulting after the removal of the solvent were consistent with the data reported in the literature for the formation of *cis*-Ru(dmpm)$_2$(H)(Ph) in ca. 50% yield.[5] This result contrasts remarkably with attempts to study the photochemical reaction of Ru(depe)$_2$H$_2$ with benzene.[3] In that case, no evidence of the phenyl hydride complex was observed, even on prolonged photolysis.

X-ray Determination of the Structure of *cis*-Ru(dmpm)$_2$H$_2$. An X-ray quality crystal of *cis*-Ru(dmpm)$_2$H$_2$ was obtained from a concentrated hexane solution at −20 °C. The compound crystallized in the space group P2$_1$/*c*. An ORTEP drawing of the dihydride is shown in Figure 8. Selected bond lengths and angles are listed in Tables 2 and 3. The molecular structure of *cis*-Ru(dmpm)$_2$H$_2$ is approximately octahedral with the two hydride ligands located in mutually *cis*-posi-

Table 3. Selected Bond Distances (Å) and Angles (deg) for *cis*-Ru(dmpm)$_2$H$_2$ (Enantiomer 2)

Ru(2)−P(5)	2.284(2)	P(6)−C(13)	1.845(6)
Ru(2)−P(6)	2.299(2)	P(6)−C(14)	1.846(6)
Ru(2)−P(7)	2.283(2)	P(6)−C(15)	1.834(6)
Ru(2)−P(8)	2.312(2)	P(7)−C(16)	1.828(7)
Ru(2)−H(3)	1.60(5)	P(7)−C(17)	1.839(6)
Ru(2)−H(4)	1.52(6)	P(7)−C(18)	1.823(6)
P(5)−C(11)	1.824(7)	P(8)−C(17)	1.857(6)
P(5)−C(12)	1.835(7)	P(8)−C(19)	1.832(6)
P(5)−C(13)	1.854(6)	P(8)−C(20)	1.833(6)
P(5)−Ru(2)−P(6)	72.04(7)	H(3)−Ru(2)−P(5)	92(2)
P(5)−Ru(2)−P(7)	179.39(6)	H(3)−Ru(2)−P(6)	160(2)
P(5)−Ru(2)−P(8)	107.56(8)	H(3)−Ru(2)−P(7)	88(2)
P(6)−Ru(2)−P(7)	107.64(7)	H(3)−Ru(2)−P(8)	88(2)
P(6)−Ru(2)−P(8)	108.10(7)	H(4)−Ru(2)−P(5)	87(2)
P(7)−Ru(2)−P(8)	72.01(7)	H(4)−Ru(2)−P(6)	86(2)
P(6)−C(13)−P(5)	93.5(2)	H(4)−Ru(2)−P(7)	93(2)
P(7)−C(17)−P(8)	93.9(3)	H(4)−Ru(2)−P(8)	162(2)

tions. The average Ru−H distance is 1.56 Å. The average length of the Ru−P bonds *trans* to the hydrogen atoms (2.304(2) Å) exceeds the average for the two other Ru−P bonds (2.282(2) Å), in accordance with the *trans*-influence of the hydride ligands. The average P−Ru−P angle is 72.03(7)° within the four-membered ring. The mutually *trans* phosphorus atoms are almost colinear, with average P−Ru−P angles of 179.23(6)°. The remaining P−Ru−P angle averages 108.04(7)°.

Discussion

The photochemistry of *cis*-Ru(dmpm)$_2$H$_2$ follows the same pattern as the related compound Ru(dmpe)$_2$H$_2$. Hydrogen is eliminated on photolysis, and the four-coordinate species Ru(dmpm)$_2$ is formed. The unsaturated fragment reacts readily to reform the dihydride in the presence of added H_2. The 16-electron complex can also be trapped by other substrates.

Spectrum and Structure. The UV−vis spectrum of Ru(dmpm)$_2$ obtained in argon matrices (Figure 1a) shows weak bands at 240, 340, 440, and 570 nm. We have recently demonstrated that Ru(dmpe)$_2$, Ru(depe)$_2$, and Ru(dppe)$_2$ have square-planar structures, which are associated with the three prominent bands between 400 and 800 nm in their UV−vis spectra.[3] This conclusion is based on comparison with the isoelectronic ion [Rh(dppe)$_2$]$^+$, which has been shown to adopt a structure close to square-planar by X-ray crystallography.[13] The UV−vis spectrum of the Rh cation[14] also contains three bands, although their position are shifted 10000−12000 cm^{-1} to higher energy compared to those of Ru^0 analogues. The UV−vis spectra of Ru(dmpe)$_2$, Ru(depe)$_2$, and Ru(dppe)$_2$ are very similar, in spite of the changes in the donor properties of the phosphines. In contrast to these complexes, Ru(dmpm)$_2$ does not display a clear multiband pattern characteristic of Ru(drpe)$_2$, although weak absorbances are still observed in the visible part of the spectrum. The low-energy band for Ru(dmpm)$_2$ lies at 570 nm and is blue-shifted ca. 4150 cm^{-1} compared to that of Ru(dmpe)$_2$.[15] The medium- and high-energy bands are also shifted to higher energy by 4850 and 7800 cm^{-1}, respectively. Since the difference in donor properties between dmpe and dmpm must be smaller than that between dmpe and depe, it is likely to be the strain induced by the four-membered ring of the metal−ligand system which causes the alteration in the spectrum. The bite angle P−Ru−P for the dmpm ligand in the dihydride *cis*-Ru(dmpm)$_2$H$_2$ is ca. 72°. This value agrees with those found in the literature for the complexes [Ru$_3$(μ-dmpm)$_3$(dmpm)$_3$Cl$_6$]-C_7H_8·C_2H_5OH (71.1(1)°)[9] and *trans*-[Ru(dmpm)$_2$(η^1-dmpm)H]PF$_6$ (72(2)°).[8] A mean bite angle of 84° for the dmpe ligand has been derived from the crystallographic data of several Ru−dmpe complexes reported by Burn et al.[16] The dramatic change observed in the UV−vis spectrum of Ru(dmpm)$_2$ compared to that of Ru(dmpe)$_2$ may be explained by the compression of 12° in the P−Ru−P angles while maintaining a planar RuP_4 skeleton. In contrast, Ru(dppe)$_2$ has a low-energy absorption band similar to Ru(dmpe)$_2$, and the bite angle of dppe[6] is only about 1° different from that of dmpe.

The transient UV−vis spectrum of Ru(dmpm)$_2$ recorded in heptane solutions after flash photolysis is similar in pattern to that obtained in low-temperature matrices, although the bands appear to be shifted. The long-wavelength band maximum lies at 530 nm in solution but at 570 nm in the matrix. The matrix spectrum shows bands at 330 and 430 nm in addition, whereas the solution spectrum just shows a shoulder at 380 nm. A change in the solvent from heptane to benzene causes a more pronounced blue shift in the spectrum observed on flash photolysis of Ru(dmpm)$_2$H$_2$ with the λ_{max} of the low-energy band appearing at 480 nm. This shift is attributed to the formation of the arene complex Ru(dmpm)$_2$(η^2-C_6H_6) in neat benzene (see below).

Reactivity. The difference found in the structure for Ru(dmpm)$_2$ compared to that of Ru(dmpe)$_2$ contrasts with the similarity in reactivity toward most of the reagents. The rate constant for the oxidative addition of H_2 to Ru(dmpm)$_2$ is found to be 4.9×10^8 dm^3 mol^{-1} s^{-1}. This value is close to that of 4.0×10^8 dm^3 mol^{-1} s^{-1} found for Ru(depe)$_2$, although it is more than an order of magnitude smaller than that obtained for Ru(dmpe)$_2$ ($k_2 = 6.8 \times 10^9$ dm^3 mol^{-1} s^{-1}). Ru(dmpm)$_2$ also reacts with CO, C_2H_4, and Et_3SiH with rate constants (Table 1) similar to that for the H_2 reaction, showing no preference for any particular ligand. This result differs from the trend observed for Ru(dmpe)$_2$, Ru(depe)$_2$, and Ru(dppe)$_2$ for which the reactivity increases with substrate in the order C_2H_4 < CO < H_2. A complete set of values for Ru(dmpm)$_2$, Ru(dmpe)$_2$, and Ru(depe)$_2$ appears in Table 1.

In the absence of H_2 or other added ligands, the decay of Ru(dmpm)$_2$ in alkane solutions follows pseudo-first-order kinetics, suggesting reaction with the precursor or the solvent or an intramolecular process. The latter is very unlikely as the four-membered ring of the metal−ligand system would prevent intramolecular C−H additions. The pseudo-first-order rate constant for the decay of Ru(dmpm)$_2$ in heptane, $k_{obs} = 1.4 \times 10^5$ s^{-1}, is three times greater than that in cyclohexane ($k_{obs} = 4.7 \times 10^4$ s^{-1}), but this difference lies within the range of general solvent effects. It is most likely that the

(13) Hall, M. C.; Kilbourn, B. T.; Taylor, K. A. *J. Chem. Soc. A*, **1970**, 2539.

(14) Geoffroy, G. L.; Isci, H.; Litrenti, J.; Mason, W. R. *Inorg. Chem.* **1977**, *16*, 1950.

(15) UV−vis band maxima for Ru(dmpe)$_2$ in cyclohexane solution (nm): 467, 555, 745.[2]

(16) Burn, M. J.; Fickes, M. G.; Hollander, F. J.; Bergman, R. G. *Organometallics* **1995**, *14*, 137.

kinetic behavior observed in alkane solvents results from a composite effect of the reaction of Ru(dmpm)$_2$ with the dihydride precursor and competing recombination with H_2.

The reaction in benzene appears to be complex. The addition of C_6H_6 to heptane solutions of *cis*-Ru(dmpm)$_2$H$_2$ causes a decrease in the rate constant for the decay of the transient species with respect to that in neat heptane. Saturation behavior is observed when the concentration of benzene exceeds 0.1 mol dm^{-3}. Under these conditions, the observed decay of the transient is at its *slowest*. The kinetic isotope effect (k_H/k_D) for the reaction of Ru(dmpm)$_2$ with neat benzene and benzene-d_6 is found to be 1.8, suggesting that the slow reaction involves C−H bond breaking in its transition state leading to formation of the phenyl hydride complex. The observed kinetics can be explained in terms of a rapid pre-equilibrium step between Ru(dmpm)$_2$ and the arene complex Ru(dmpm)$_2$(η^2-C_6H_6). The latter undergoes oxidative addition of benzene relatively slowly, leading to the phenyl hydride species (Scheme 1). We define two rate constants in Scheme 1. The pseudo-first-order rate constant k_1 corresponds to the composite reaction observed in pure heptane. The benzene complex, Ru(dmpm)$_2$(η^2-C_6H_6), is formed with an equilibrium constant K and is converted to phenyl hydride complex with a first-order rate constant k_2.

The kinetic analysis of Scheme 1 can be simplified. The rate constant for the C−H activation reaction, k_2, can be obtained from the measurements at high benzene concentrations as ca. 3.5×10^3 s^{-1}. Since this value is far less than k_1 (ca. 10^5 s^{-1}), k_2 has not been included in the analysis shown below for low [C_6H_6], where M = Ru(dmpm)$_2$.

$$K = [M(C_6H_6)]/[M][C_6H_6] \quad (1)$$

We define [M_{tot}] as

$$[M_{tot}] = [M] + [M(C_6H_6)] \quad (2)$$

so [$M(C_6H_6)$] = [M_{tot}] − [M], and substituting into eq 1 and rearranging

$$[M] = [M_{tot}]/\{K[C_6H_6] + 1\} \quad (3)$$

the rate of depletion of [M] is k_1[M]

$$\text{rate} = k_1\,[M_{tot}]/\{K[C_6H_6] + 1\} \quad (4)$$

hence

$$k_{obs} = k_1/\{K[C_6H_6] + 1\} \quad (5)$$

$$1/k_{obs} = \{K[C_6H_6] + 1\}/k_1 \quad (6)$$

Thus, a plot of $1/k_{obs}$ against [C_6H_6] should give a straight line (Figure 7) with a slope of K/k_1 and an intercept of $1/k_1$. The equilibrium constant K can be determined from the ratio of the slope to intercept and is found to be 290 ± 70.[17] A k_1 value of (1.0 ± 0.3) × 10^5 s^{-1} is obtained from the analysis. This is consistent with the k_{obs} value measured in pure heptane of 1.5×10^5 s^{-1}.

Scheme 1. Kinetic Scheme for the Reaction of Ru(dmpm)$_2$H$_2$ in Heptane/Benzene Mixtures

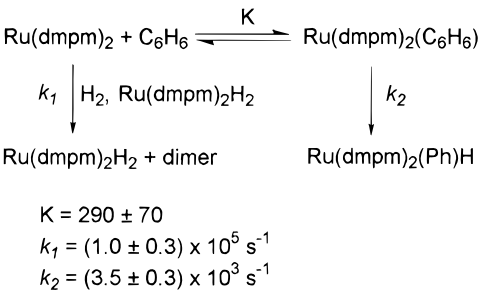

Scheme 2. Transient Photochemistry of Ru(dmpm)$_2$H$_2$ in Solution at Ambient Temperature

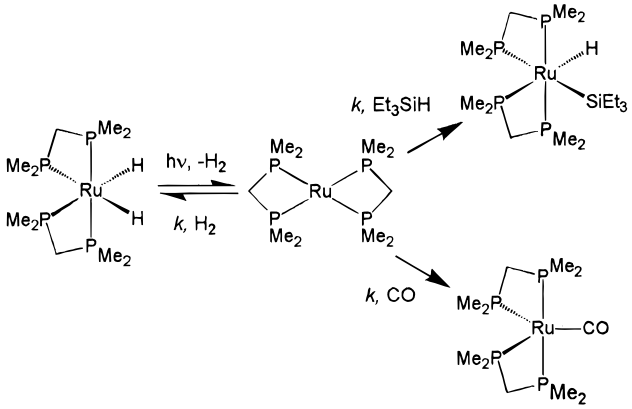

It is interesting to compare Ru(dmpm)$_2$ to Ru(dmpe)$_2$, which shows no reaction with benzene in flash photolysis experiments. Care is needed with this comparison because Ru(dmpe)$_2$ decays in benzene by recombination with expelled H_2 following second-order kinetics, whereas Ru(dmpm)$_2$ decays by first-order kinetics. We therefore consider the value of k_2/ϵl for Ru(dmpe)$_2$ (i.e., the slope of the second-order plot), where k_2 is the second order rate constant for reaction with H_2, ϵ the extinction coefficient, and l the path length. The measured value of k_2/ϵl is 2.8×10^6 s^{-1}, 30 times greater than the first-order rate constant obtained for Ru(dmpm)$_2$ (1×10^5 s^{-1}). As a result of this factor, the reaction of Ru(dmpe)$_2$ in C_6H_6 proceeds almost exclusively via the route of recombination with H_2. If the conversion of Ru(dmpe)$_2$(C_6H_6) to Ru(dmpe)$_2$(Ph)H is relatively slow, as for the dmpm complex, we can deduce that the value of the corresponding equilibrium constant, K, for Ru(dmpe)$_2$ (as in Scheme 1) is less than 0.1.[18]

In contrast, Fe(dmpe)$_2$ is observed to react with arenes by flash photolysis.[2a] Although the mechanism proposed for the arene activation is very similar to that represented in Scheme 1, for Fe(dmpe)$_2$, $k_1 \ll k_2$ whereas for Ru(dmpm)$_2$, $k_2 \ll k_1$. The equilibrium constant, K, is much smaller for Fe(dmpe)$_2$ than for Ru(dmpm)$_2$.

Conclusions

The transient photochemistry of *cis*-Ru(dmpm)$_2$H$_2$ is summarized in Schemes 1 and 2. Ru(dmpm)$_2$ is gener-

(17) The requirements of a fast equilibrium would be satisfied if the rate constant for formation of Ru(dmpm)$_2$(C_6H_6) from Ru(dmpm)$_2$ + C_6H_6 is ca 3×10^8 dm^3 mol^{-1} s^{-1} and the reverse rate constant is ca. 10^6 s^{-1}, when [C_6H_6] ≥ 10^{-2} mol dm^{-3}. This limitation includes all of the points of Figure 7, except those close to the origin.

(18) The kinetic behavior of Ru(dmpe)$_2$ is not affected measurably by the addition of 1 mol dm^{-3} C_6H_6 to a cyclohexane solution. If we assume that k_{obs} is changed by less than 10%, inspection of the denominator of eq 5 indicates a limiting value of $K \leq 0.1$.

Table 4. Crystal Data for *cis*-Ru(dmpm)$_2$H$_2$

empirical formula	$C_{20}H_{60}P_8Ru_2$
fw	750.58
cryst syst	monoclinic
habit, color, dimensions	colorless block, 0.80 × 0.40 × 0.40 mm^3
temp	293(2) K
lattice params	a = 12.110(10) Å
	b = 18.653(7) Å
	c = 17.509(10) Å
	β = 109.66(6)°
	V = 3724(4) Å^3
space group	$P2_1/c$ (No. 14)
Z	4
D_{calcd}	1.339 g cm^{-3}
F_{000}	1552
diffractometer	Rigaku AFC6S
radiation	Mo Kα (λ = 0.7107 Å), graphite-monochromated
transmission coefficients	0.89 (min), 1.00 (max), determined from average of 10 azimuthal scans
linear attenuation coefficient, μ(Mo Kα)	1.163 mm^{-1}
scan type	$\omega-2\theta$
θ range	2.51−25.01°
index ranges	$0 \le h \le 14$, $0 \le k \le 22$, $-20 \le l \le 19$
no. of rflns meas	7129
no. of indep rflns	6791 (R_{int} = 0.051)[a]
data/restraints/param	6514/0/303
refln/param ratio	21.5
goodness of fit indicator on F^2	1.068
residuals, R[b]	
$[I_o > 2\sigma(I_o)]$ 4950 data	R1 = 0.0375, wR2 = 0.0908
all data	R1 = 0.0688, wR2 = 0.2342
max peak in final diff map	0.49 e Å^{-3}
min peak in final diff map	−0.50 e Å^{-3}

[a] $R(\text{int}) = \sum|F_o^2 - F_o^2(\text{mean})|/\sum(F_o^2)$. [b] $R1 = \sum||F_o| - |F_c||/\sum|F_o|$, $wR2 = \{\sum[w(F_o^2 - F_c^2)^2]/\sum[w(F_o^2)^2]\}^{1/2}$.

ated upon photolysis of the dihydride complex *cis*-Ru(dmpm)$_2$H$_2$. The UV−vis spectra of Ru(dmpm)$_2$ obtained in solution at 295 K and in matrices at 12 K do not exhibit the three-band pattern characteristic for Ru(drpe)$_2$ (drpe = dmpe, depe, dppe) but do retain an absorption band between 500 and 600 nm. We postulate that Ru(dmpm)$_2$ has a planar RuP$_4$ skeleton of D_{2h} symmetry and that the UV−vis spectra are sensitive to variation in the bite angle P−Ru−P, which is reduced from ca. 84° in Ru(dmpe)$_2$ to ca. 72° in Ru(dmpm)$_2$. Reaction with benzene is observed by laser flash photolysis. The kinetics are explained by assuming a fast equilibrium between Ru(dmpm)$_2$ and the arene complex Ru(dmpm)$_2$(η^2-C$_6$H$_6$) and a much slower conversion to the phenyl hydride complex Ru(dmpm)$_2$(Ph)H. Ru(dmpm)$_2$ reacts with H$_2$, CO, C$_2$H$_4$, and Et$_3$SiH with similar rate constants to those of Ru(dmpe)$_2$ but proves to be less selective.

Experimental Section

General Methods and Materials. Ruthenium trichloride was obtained as a loan from Johnson Matthey, and dmpm was obtained from Strem. Triethylsilane was purchased from Aldrich and stored over activated 3 Å molecular sieves. Ru(dmpm)$_2$H$_2$ was prepared by literature procedures.[5] The hydride region of the ^{1}H NMR spectrum showed resonances for the *cis*-isomer at δ −8.11 and for the *trans*-isomer at δ −6.15 in a ratio of at least 80:1. Compounds were synthesized and handled using standard Schlenk, high-vacuum, and glovebox techniques. Solvents for synthesis (AR grade) were dried by refluxing over sodium/benzophenone (hexane, benzene, toluene, THF, Et$_2$O) or P$_2$O$_5$ (CH$_2$Cl$_2$) and then distilled under an argon atmosphere, while solvents for flash photolysis (Aldrich, HPLC grade) were refluxed over calcium hydride under argon. Benzene-d_6 and THF-d_8 (Goss Scientific Instrument, Ltd.) were dried by stirring over potassium/benzophenone and then vacuum transferred. Gases used for the matrix experiments (Ar, CH$_4$) and for the flash experiments (Ar, H$_2$, CO, C$_2$H$_4$) were BOC research grade (99.999% purity).

Matrix Isolation Experiments. The matrix isolation apparatus is described in detail elsewhere.[19] Samples for IR spectroscopy alone were deposited onto a CsI window cooled by an Air Products CS202 closed-cycle refrigerator to 12−25 K. A BaF$_2$ window was used for combined IR and UV−vis spectroscopy. The outer windows of the vacuum shroud were chosen to match. Ru(dmpm)$_2$H$_2$ was sublimed from right-angled glass tubes (at 333 K) at the same time as a gas stream entered the vacuum shroud. Temperatures and rates of deposition were 20 K for Ar (2 mmol h^{-1}) and 25 K for CH$_4$ (2 mmol h^{-1}). The samples were cooled to 12 K before recording the IR spectra on a Mattson Unicam Research Series FTIR spectrophotometer fitted with a TGS detector and a CsI beam splitter, which was continuously purged with dry CO$_2$-free air. Spectra were recorded at 1 cm^{-1} resolution with 128 scans coaveraged (25 K data points with two-times zero filling). UV−vis spectra were recorded on the same sample at the same temperature on a Perkin-Elmer Lambda 7G spectrophotometer. Matrices were photolyzed through a quartz window with an ILC 302UV 300 W Xe arc equipped with either UV-reflecting (200−400 nm) or visible-reflecting (400−800 nm) mirrors and a water filter. Photolysis wavelengths were selected with cutoff or interference filters.

Laser Flash Photolysis. The apparatus for flash photolysis experiments has been described in detail elsewhere.[2] Briefly, a XeCl excimer laser (308 nm) is used as the excitation source, and a Xe arc lamp is used as a monitoring source. The Xe arc is pulsed for measurements on short time scales (<250 μs), and otherwise the Xe arc is used in a continuous mode. The spectrometer is linked to a digital oscilloscope (Tektronix TDS 520), and the system is controlled by a PC. Transient signals are usually collected as 12- or 16-shot averages.

Samples of Ru(dmpm)$_2$H$_2$ for flash experiments were sublimed immediately before use and handled in the glovebox

(19) Haddleton, D. M.; McCamley, A.; Perutz, R. N. *J. Am. Chem. Soc.* **1988**, *110*, 1810.

exclusively. The samples were loaded into a quartz cuvette (10-mm path length) fitted with a Young's PTFE stopcock and degassing bulb. Solvent was added via cannula under argon on a Schlenk line fitted with a diffusion pump. The sample was degassed three times by freeze−pump−thaw cycles before being back-filled to 760 Torr with the appropriate gas. Gas mixtures were made up manometrically in 1-L bulbs such that the total pressure in the cell was typically 760 Torr. Liquid quenchers were added with a microliter syringe. The absorbances of the sample were typically 0.5−1.0 at 308 nm. Variable temperature measurements were made by replacing the standard cell holder by an insulated holder mounted on a block through which thermostated water was passed. Decays have been analyzed by linear least-squares regression methods after conversion to absorbance using inhouse software or by fitting the decays using Microcal Origin software. The error bars on the second-order rate constants are quoted as 95% confidence limits.

NMR Spectroscopy. The NMR spectra were recorded with either a Bruker MSL 300, Bruker AMX 500, or JEOL 270 spectrometer. The ^{1}H NMR chemical shifts were referenced to residual C_6D_5H at δ 7.13. The $^{31}P\{^1H\}$ NMR chemical shifts were referenced externally to H_3PO_4 at $\delta = 0$.

Photolysis of Ru(dmpm)$_2$H$_2$ in Et$_3$SiH. *cis*-Ru(dmpm)$_2$H$_2$ (20 mg, 0.05 mmol) was dissolved in a mixture of hexane: Et_3SiH (1.5:0.5 mL) and photolyzed in an ampule with a Philips HPK 125-W medium-pressure mercury arc and water filter for ca. 5 h. Removal of the solvent and analysis of the residue by NMR spectroscopy showed the formation of *cis*-Ru(dmpm)$_2$(SiEt$_3$)H in 85% yield.

cis-Ru(dmpm)$_2$(Et$_3$Si)H: ^{1}H NMR (benzene-d_6, 270 MHz) δ −8.81 (dq, Ru*H*, J_{trans} = 68.2 Hz, J_{cis} = 20.4 Hz), 0.52 (q, RuSiC*H*$_2$CH$_3$, J_{HH} = 7.9 Hz), 1.54 (t, RuSiCH$_2$C*H*$_3$, J_{HH} = 7.9 Hz), 1.0−1.5 (m, PC*H*$_3$), 3.0−3.4 (m, PC*H*$_2$P). $^{31}P\{^1H\}$ NMR (benzene-d_6, 109.3 MHz) δ −19.3 (P_A), −25.5 (P_B), −33.8 (P_M), −5.1 (P_Q) (J_{AB} = 255.3, J_{AM} = 56.3 Hz, J_{AQ} = 37.6 Hz, J_{BM} = 32.9 Hz, J_{BQ} = 61.0 Hz).

X-ray Structure of *cis*-Ru(dmpm)$_2$H$_2$. Crystals of the dihydride suitable for single-crystal X-ray diffraction were obtained by recrystallization from hexane at 253 K. A brief summary of crystallographic details is given in Table 4. Selected bond lengths and angles are given in Tables 2 and 3. The structure was solved using Patterson methods with SAPI9[20] and expanded using Fourier techniques with DIRDIF.[21] The structure was refined using full-matrix least-squares on F^2 with SHELXL93.[22] All non-hydrogen atoms were refined anisotropically. The hydrides H(1), H(2), H(3), and H(4) were located in a Fourier difference map and were refined isotropically. All other hydrogen atoms were refined using a rigid model: $C_{sp^3}(CH_3)-H$ = 0.96 Å, $C_{sp^3}(CH_2)-H$ = 0.97 Å with $U_{iso}\{H[C_{sp^3}(CH_3)-H]\} = 1.5\ U_{eq}(C_{sp^3})$, $U_{iso}\{H[C_{sp^3}(CH_2)-H]\} = 1.2\ U_{eq}(C_{sp^3})$. The asymmetric unit contains the two enantiomers related by an apparent center of symmetry. Accordingly, the lattice was checked carefully for higher symmetry, revealing a near C-centered orthorhombic cell (γ = 90.57°). However, a precession-photograph simulation of the data did not have the appropriate Laue symmetry, and this higher symmetry cell was rejected. The monoclinic cell, based on the near C-centered orthorhombic cell, was also tested for possible twinning by applying the appropriate twin-law matrix to the data. Refinement of the BASF parameter in SHELXL93 indicated that no twinning was present. The structure is displayed in Figure 8 with the ORTEP routine.[23] Structure searches were carried out on the Cambridge structural database.[24]

Acknowledgment. We acknowledge the European Commission for financial support. We are extremely grateful to Dr D. Dukic for his help in interfacing and development of the software for the flash photolysis apparatus and to Mr. D. Pattison for helpful discussions. We also acknowledge the help of Mr L. Cronin with the X-ray crystallography.

Supporting Information Available: X-ray crystallographic data on *cis*-Ru(dmpm)$_2$H$_2$, including tables of atomic coordinates, bond lengths and angles, anisotropic displacement parameters, hydrogen coordinates and U_{eq}, and packing diagram (10 pages). Ordering information available on any current masthead page.

OM961018E

(20) Hai-Fu, F. *Structure Analysis Programs with Intelligent Control*; Rigaku Corporation: Tokyo, Japan, 1993.
(21) Beurskens, P. T.; Admiraal, G.; Beurskens, G.; Bosman, G.; Garcia-Granda W. P.; Gould, R. O.; Smiths, J. M. M.; Smykall, C. *The DIRDIF Program System. Technical Report of the Crystallography Laboratory*; University of Nijmegen: The Netherlands, 1992.
(22) Sheldrick, G. M. *SHELXL93. Program for crystal structure refinement*. University of Göttingen: Germany, 1993.
(23) Johnson, C. K. *ORTEP Report ORNL-5138*; Oak Ridge National Laboratory: Oak Ridge, TN, 1976.
(24) Fletcher, D. A.; McMeeking, R. F.; Parkin, D. J. *J. Chem. Inf. Comput. Sci.* **1996**, *36*, 746.